PREPRINT 480

JUNE 2018

Well-balanced scheme for gas-flow in pipeline networks

Yogiraj Mantri[1], Michael Herty[1] and Sebastian Noelle[1]

Institut für Geometrie und Praktische Mathematik
Templergraben 55, 52062 Aachen, Germany

[1] IGPM, RWTH Aachen University, Templergraben 55, D-52062 Aachen, Germany

Well-balanced scheme for gas-flow in pipeline networks

Yogiraj Mantri[1], Michael Herty[1], and Sebastian Noelle[1]

[1]*IGPM, RWTH Aachen University, Templergraben 55, 52056 Aachen, Germany.*

Abstract

Gas flow through pipeline networks can be described using 2×2 hyperbolic balance laws along with coupling conditions at nodes. The numerical solution at steady state is highly sensitive to these coupling conditions and also to the balance between flux and source terms within the pipes. To avoid spurious oscillations for near equilibrium flows, it is essential to design well-balanced schemes. Recently Chertock, Herty & Özcan [11] introduced a well-balanced method for general 2×2 systems of balance laws. In this paper, we extend this approach to a network of pipes. We prove well-balancing for different coupling conditions and for compressors stations, and demonstrate the advantage of the scheme by numerical experiments.

1 Introduction

The study of mathematical models for gas flow in pipe networks has recently gained interest in the mathematical community, see e.g. [3,4,9,14,26]. While in the engineering literature [30] the topic has been discussed some decades ago, a complete mathematical theory has only emerged recently, see e.g. [16] for the Euler system on networks, [12] for the p–system on networks and [8] for a recent review article on general mathematical models on networks. Depending on the scale of phenomena of interest, different mathematical models for gas flow might be useful. A complete hierarchy of fluid–dynamic models has been developed and discussed in [9]. Therein, typical flow rates and pressure conditions are given and it is shown that a steady state algebraic model can be sufficient to describe average states in a gas network. Models based on an asymptotic expansion of the pressure may lead to further improvements in case of typical, slowly varying, temporal flow patterns [18, 22]. If a finer resolution of the spatial and temporal dynamics is required, the isothermal Euler equations (1.1) provide a suitable model [3]. Here we focus on schemes which capture both steady states and small temporal and spatial perturbations.

Schemes which preserve a steady state exactly are called well-balanced, and their development is a lively topic in the field of hyperbolic balance laws, see e.g. the monograph [31]. Usually, these schemes use specific knowledge of an equilibrium state. As a consequence, well-balanced schemes for still water such as [1, 28], or for moving water, [29], or for wet-dry fronts such as [6, 10], which all approximate solutions to the shallow water equations, use different discretization techniques. A unified approach to well-balancing in one space dimension was recently proposed by Chertock et al. [11], who integrate the source term in space and substract it from the numerical flux. They tested their scheme for subsonic gas flow in a pipe with wall friction. To the best of our knowledge, there is currently no well–balanced scheme

for hyperbolic flows on **networks**. Here spurious oscillations may not only be caused by an imbalance of numerical fluxes and source terms, but also by discretization errors at junctions and compressors. In the present paper, we develop a first order well-balanced scheme on a network. High-order schemes for gas networks have been introduced only recently in [2,7,27]. A challenging question would be to extend our new well-balancing method to these more accurate schemes.

In the following we introduce the mathematical model for the temporal and spatial dynamics of gas flow in pipe networks. For simplicity, we study a single node $x = x_o$ where M pipes meet. The flow within each pipe $i = 1 \dots M$ is governed by the isothermal Euler equations

$$(U_i)_t + F(U_i)_x = S(U_i) \tag{1.1}$$

with conservative variables U_i, flux $F(U_i)$ and source $S(U_i)$ given by

$$U_i = \begin{bmatrix} \rho_i \\ q_i \end{bmatrix}, \; F(U_i) = \begin{bmatrix} q_i \\ \frac{q_i^2}{\rho_i} + p(\rho_i) \end{bmatrix}, \; S(U_i) = \begin{bmatrix} 0 \\ -\frac{f_{g,i}}{2D_i} \frac{q_i|q_i|}{\rho_i} \end{bmatrix}. \tag{1.2}$$

Here ρ_i, q_i and $p(\rho_i)$ are the density, momentum, and pressure of the gas, $f_{g,i}$ is the friction factor and D_i the diameter of pipe i. We focus on the practically relevant case of isothermal pressure with speed of sound $a > 0$,

$$p(\rho) = \rho RT = a^2 \rho. \tag{1.3}$$

We complete (1.1) with initial conditions within and boundary conditions at the ends of the pipes. The boundary conditions at a node of multiple pipes are implicitly given by coupling conditions [3,34], which take the form of M nonlinear algebraic equations involving traces U_i of the conserved variables at node x_o. We write them in the general form

$$\phi(U_1, U_2, ..., U_M) = 0, \quad \phi : \mathbb{R}^{2M} \to \mathbb{R}^M. \tag{1.4}$$

In [14,15,34] general conditions are identified which guarantee a well–posed problem for initial data with suitable small total variation. If at a node the conservation of mass and equality of adjacent pressures is assumed, then existence, uniqueness and continuous dependence on the initial data for the p–system was shown in [13].

For pipes with a junction, a flow which is steady within each pipe, and fulfills the coupling conditions at the junction is called a steady state [21]. The coupling conditions are further detailed in Sections 2 and 3.

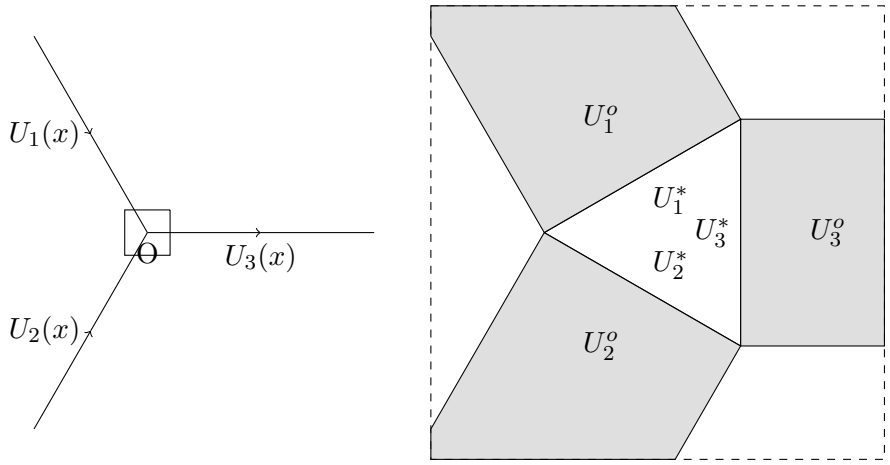

Figure 1: Intersection of three pipes at junction O. Right- Zoomed view of the junction with old traces U_i^o and new traces U_i^* given in Section 2

2 Review of coupling conditions for the p–system

Our construction of well–balanced schemes is based upon analytical results for the isothermal Euler equations which have already been established (see e.g. [3,13] and the references therein). For completeness, and to fix the notation, we would like to give a brief summary.

When we study the coupling condition, we set the source terms $S(U_i)$ to zero. This is based on the heuristic assumption that wall friction can be neglected at the instance of interaction at the node. It can also be justified rigorously for the semi-discrete scheme (4.1). The eigenvalues for the homogeneous 2×2 system (1.1) are $\lambda_1 = \frac{q}{\rho} - a$ and $\lambda_2 = \frac{q}{\rho} + a$. We assume that all states are **subsonic**, i.e.,

$$\lambda_1(U_i) < 0 < \lambda_2(U_i) \quad \text{for } i = 1 \dots M. \tag{2.1}$$

This assumption is satisfied for typical gas flow conditions in high–pressure gas transmission systems. We denote the set of all incoming (respectively outgoing) pipes by I^- (respectively I^+). For $i \in I^-$, we parametrize the incoming pipes by

$$x \in \Omega_i := (-\infty, x_o).$$

Similarly, we parametrize outgoing pipes $j \in I^+$ by

$$x \in \Omega_j := (x_o, \infty).$$

Let us fix a time $t_o \geq 0$. It is important to note that there are $2M$ different traces at the node (x_o, t_o). We denote them by

$$U_i^o := \lim_{x \uparrow x_o} \lim_{t \downarrow t_o} U_i(x,t) \quad \text{for } i \in I^-, \tag{2.2}$$

$$U_i^* := \lim_{t \downarrow t_o} \lim_{x \uparrow x_o} U_i(x,t) \quad \text{for } i \in I^-, \tag{2.3}$$

$$U_j^o := \lim_{x \downarrow x_o} \lim_{t \downarrow t_o} U_j(x,t) \quad \text{for } j \in I^+. \tag{2.4}$$

$$U_j^* := \lim_{t \downarrow t_o} \lim_{x \downarrow x_o} U_j(x,t) \quad \text{for } j \in I^+, \tag{2.5}$$

Note that the limits are exchanged in (2.3) and (2.2) (respectively (2.5) and (2.4)), so U_i^o and U_j^o are limits along the x-axis. We call them the *old traces*. The states U_i^* and U_j^* are limits along the t axis, and we call them the *new traces* (see Figure 1).

The construction of the coupling conditions starts by connecting, within each pipe, the old with the new trace by a Lax curve entering the pipe. For an incoming pipe, this will be a curve $\overline{U}_i(\sigma_i)$ of the first family with left state $U_l := U_i^o$. According to [17], this curve is given by

$$1-R: \quad \overline{U}_i(\sigma_i) := \rho_l\, e^{\sigma_i} \begin{bmatrix} 1 \\ u_l - a\sigma_i \end{bmatrix} \quad \text{for } \sigma_i \geq 0, \tag{2.6}$$

$$1-S: \quad \overline{U}_i(\sigma_i) := \rho_l(1+\sigma_i) \begin{bmatrix} 1 \\ u_l - \frac{a\sigma_i}{\sqrt{1+\sigma_i}} \end{bmatrix} \quad \text{for } \sigma_i \in (-1,0). \tag{2.7}$$

Analogously, for an outgoing pipe, we use curves of the second family with right state $U_r := U_j^o$, which are given by

$$2-R: \quad \overline{U}_j(\sigma_j) := \rho_r\, e^{\sigma_j} \begin{bmatrix} 1 \\ u_r + a\sigma_j \end{bmatrix} \quad \text{for } \sigma_j \leq 0, \tag{2.8}$$

$$2-S: \quad \overline{U}_j(\sigma_j) := \rho_r(1+\sigma_j) \begin{bmatrix} 1 \\ u_r + \frac{a\sigma_j}{\sqrt{1+\sigma_j}} \end{bmatrix} \quad \text{for } \sigma_j > 0. \tag{2.9}$$

The Lax curves 1-R and 1-S(respectively 2-R and 2-S) have C^2 continuity at the point U_l(respectively U_r).

The parameters $\sigma_i, i = 1 \dots M$ will be determined from the M coupling conditions

$$\overline{\phi}(\sigma_1, \dots, \sigma_M) := \phi(\overline{U}_1(\sigma_1), \dots, \overline{U}_M(\sigma_M)) = 0. \tag{2.10}$$

Now we set

$$U_i^* := \overline{U}_i(\sigma_i). \tag{2.11}$$

By construction, the new traces satisfy the coupling conditions (1.4).

So far, we have reviewed the general framework which was established and applied in [3,13,32]. In the following we focus on a particular coupling condition for which we design a well-balanced scheme. Let $A_i = \frac{\pi}{4} D_i^2$ be the area of the cross section of pipe i. The default coupling condition requires that the total incoming mass flux at each node x_o equals the total outgoing mass flux,

$$\sum_{i \in I^-} A_i q_i^* = \sum_{j \in I^+} A_j q_j^*, \tag{2.12}$$

since mass should not be accumulated or lost at the junction. Various approaches have been studied in order to model the other $(M-1)$ coupling conditions. A seemingly obvious choice would be conservation of momentum. However as momentum is a vector quantity it is difficult to describe the conservation of momentum in a one dimensional model as the junctions of the pipe are three dimensional. Multi–dimensional approaches considering a 2D node for a 1D flow have been discussed in [5,23]. Coupling conditions based on enthalpy have also been studied in [3, 26, 33, 34]. In the present paper, we require that the traces of the pressures should take one and the same value $p^* = p^*(t_o)$ at the t-axis,

$$p(\rho_i^*) = p^*(t_o) \quad \text{for all } i \in I^- \cup I^+. \tag{2.13}$$

This condition is common in the engineering literature and for a certain regime, it is indeed a suitable approximation of the two dimensional situation [23].

Thus the coupling function (1.4) at a junction reads

$$\phi(U_1,\dots,U_M) = \begin{bmatrix} \sum_{i\in I^-} A_i q_i - \sum_{j\in I^+} A_j q_j \\ p(\rho_2) - p(\rho_1) \\ \vdots \\ p(\rho_M) - p(\rho_{M-1}) \end{bmatrix}. \tag{2.14}$$

We now turn to a junction which models a compressor between the incoming pipe $i = 1$ and the outgoing pipe $i = 2$, both of the same diameter. The coupling conditions for the new traces are

$$q_1^* = q_2^*, \quad p(\rho_2^*) = CR\, p(\rho_1^*). \tag{2.15}$$

Here $CR \geq 1$ is the compression ratio. It is usually time–dependent, and we consider it to be a given, external quantity. Thus the coupling function for the compressor becomes

$$\phi(U_1,\dots,U_M) = \begin{bmatrix} q_2 - q_1 \\ p(\rho_2) - CR p(\rho_1) \end{bmatrix}. \tag{2.16}$$

Summarizing, the analytical problem at the nodes is to connect the old traces U_i^o within each pipe to a new trace U_i^* along the incoming Lax curve in such a way that the new traces satisfy the coupling conditions across the node. It was proven in [14, 19, 20] that this problem has a unique solution.

If the old traces are subsonic, and their variation is small enough, then the new traces will be subsonic as well. The new traces serve as initial data in the Riemann solver which determines the numerical flux.

3 Coupling conditions in terms of equilibrium variables

The difficulty in preserving steady states is that the divergence of the conservative fluxes is approximated by a flux-difference, while the source is usually integrated by a quadrature over the cell. If this is not tuned carefully, the equilibrium state is not maintained, and spurious oscillations may be created. Chertock, Herty and Özcan [11] resolved this difficulty for one-dimensional balance laws by integrating the source term and hence writing it in conservative form. They applied this approach to the Cauchy problem for 2×2 balance laws. Here we extend their method to a node in a network. Equation (1.1) can be stated as

$$(\rho_i)_t + (K_i)_x = 0,\ (q_i)_t + (L_i)_x = 0 \tag{3.1}$$

where the flux variable,

$$V_i(U_i, R_i) = \begin{bmatrix} K_i \\ L_i \end{bmatrix} = F(U_i) + \begin{bmatrix} 0 \\ R_i \end{bmatrix} \tag{3.2}$$

and fluxes K_i, L_i and an integrated source term R_i is given by

$$K_i := q_i,\ L_i := \frac{q_i^2}{\rho_i} + p(\rho_i) + R_i(x),\ R_i(x) := \int_{\tilde{x_i}}^{x} \frac{f_{g,i}}{2D_i}\, \frac{q_i|q_i|}{\rho_i}\, dx. \tag{3.3}$$

The point $\tilde{x_i}$ belongs to $\overline{\Omega}_i$ and is arbitrary but fixed. Later on, we choose $\tilde{x_i} = x_o$ for all i.

We call (K, L) the equilibrium variables, since they are constant for steady states. Given the integrated source term and the equilibrium variables we can solve equation (3.3) for the conservative variables (ρ, q). Away from sonic points, this yields a subsonic and supersonic state. The subsonic root is given by

$$\rho_i(V_i, R_i) = \frac{L_i - R_i + \sqrt{(L_i - R_i)^2 - 4K_i^2 a^2}}{2a^2},\ q_i(V_i, R_i) = K_i. \tag{3.4}$$

Rewriting the problem in terms of K and L allows to have constant steady states that are reconstructed exactly within a numerical scheme. The well–balanced finite volume scheme introduced in [11] uses the following idea: From point values of the conserved quantities (ρ, q) and a fixed point $\tilde{x}$, point values of the new variables (K, L) are computed. In order to obtain values at the cell interfaces, the new variables (K, L, R) are reconstructed *instead* of the the conservative ones. Then, the conservative variables at the cell interfaces are obtained using the transformation (3.4).

Hence, in order to extend the scheme to include the nodal dynamics we need to reformulate the coupling conditions (2.12),(2.13) in terms of equilibrium variables K, L. The pressure in terms of K, L is given by,

$$P_i = P(K_i^*, L_i^*) := \frac{L_i^* - R_i + \sqrt{(L_i^* - R_i)^2 - 4(K_i^*)^2 a^2}}{2} \tag{3.5}$$

Note that R_i appears as a parameter in P_i. Similar to the discussion in the previous section the conditions are stated for the traces of the equilibrium variables at x_o. The dependence on x_o is omitted for readability.

$$\sum_{i \in I^-} A_i K_i^* = \sum_{j \in I^+} A_j K_j^*, \tag{3.6}$$

$$P(K_i^*, L_i^*) = p^*,\ \forall i \in I^{\pm}. \tag{3.7}$$

Similarly, the coupling condition for a compressor in terms of K and L reads

$$P(K_2^*, L_2^*) = CR\, P(K_1^*, L_1^*). \tag{3.8}$$

For subsonic states, the coupling conditions (3.6),(3.7), (3.8) are equivalent to the coupling conditions (2.12),(2.13), (2.15).

For steady states, K_i and L_i are constant within each pipe, and the coupling conditions are fulfilled at the junction. Evaluating the coupling conditions in terms of the equilibrium variables $V = (K, L)$ and the parameter R is an essential ingredient of the well-balancing. Therefore, we rewrite the Lax-curves in terms of the equilibrium variables:

$$1-R: \quad \overline{V}_i(\sigma_i) := \rho_l\, e^{\sigma_i} \begin{bmatrix} u_l - a\sigma_i \\ (u_l - a\sigma_i)^2 + a^2 \end{bmatrix} + \begin{bmatrix} 0 \\ R_l \end{bmatrix} \quad \text{for } \sigma_i \geq 0, \tag{3.9}$$

$$1-S: \quad \overline{V}_i(\sigma_i) := \rho_l(1+\sigma_i) \begin{bmatrix} u_l - \frac{a\sigma_i}{\sqrt{1+\sigma_i}} \\ \left(u_l - \frac{a\sigma_i}{\sqrt{1+\sigma_i}}\right)^2 + a^2 \end{bmatrix} + \begin{bmatrix} 0 \\ R_l \end{bmatrix} \quad \text{for } \sigma_i \in (-1, 0).$$

Similarly for the admissible boundary states on the pipes $i \in I^+$ with given value R_r and $u_r = q_r/\rho_r$, we obtain

$$2-R: \quad \overline{V}_j(\sigma_j) := \rho_r\, e^{\sigma_j} \begin{bmatrix} u_r + a\sigma_j \\ (u_r + a\sigma_j)^2 + a^2 \end{bmatrix} + \begin{bmatrix} 0 \\ R_r \end{bmatrix} \quad \text{for } \sigma_j \le 0, \tag{3.10}$$

$$2-S: \quad \overline{V}_j(\sigma_j) := \rho_r(1+\sigma_j) \begin{bmatrix} u_r + \frac{a\sigma_j}{\sqrt{1+\sigma_j}} \\ \left(u_r + \frac{a\sigma_j}{\sqrt{1+\sigma_j}}\right)^2 + a^2 \end{bmatrix} + \begin{bmatrix} 0 \\ R_r \end{bmatrix} \quad \text{for } \sigma_j > 0.$$

The equilibrium variables satisfying the coupling condition (3.6) and (3.7) are given by

$$K_i^* := \overline{K}_i(\sigma_i) \text{ and } L_i^* := \overline{L}_i(\sigma_i). \tag{3.11}$$

Note that all variables defined along the Lax-curves also depend on the old traces and the integrated source terms as parameters, e.g. $\overline{V}_i(\sigma_i) = \overline{V}_i(\sigma_i; V_i^o, R_i^o)$. For given datum U_l, U_r we depict the parameterized wave curves for incoming and outgoing pipes in the phase space of K and L, respectively, in Figure 2. From the figure we observe that in the subsonic region,

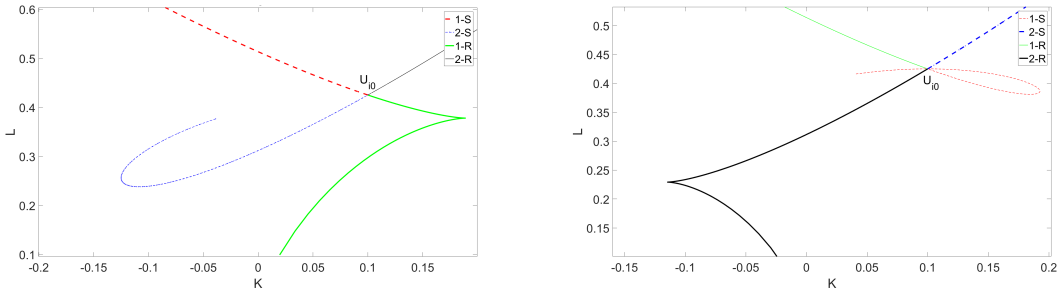

(a) Incoming pipes, $i \in I^-$ (b) Outgoing pipes, $i \in I^+$

Figure 2: Phase plot in terms of equilibrium variables

the 1–Lax curve is monotonically decreasing and 2–Lax curves is monotonically increasing. The following lemma proves that the coupling conditions stated in the variables K and L locally have a unique solution.

Lemma 3.1. *Consider a nodal point with $|I^-| \ge 1$ incoming and $|I^+| \ge 1$ outgoing adjacent pipes. Suppose that the initial data $\widehat{U}_i = (\hat{\rho}_i, \hat{q}_i)$, $i \in I^\pm$ are subsonic on each pipe and fulfill the coupling conditions (2.12) and (2.13). Let $\widehat{V}_i = (\widehat{K}_i, \widehat{L}_i), i \in I^\pm$ be the corresponding equilibrium variables, with integrated source terms $\widehat{R}_i$.*

Then there exists an open neighborhood $\mathcal{V} \subset \mathbb{R}^{2M \times M}$ of $(\widehat{V}, \widehat{R}) := (\widehat{V}_i, \widehat{R}_i)_{i \in I^\pm}$ such that for any old trace $(V^o, R^o) \in \mathcal{V}$ there exists a unique new trace V^* such that $(V^*, R^o) \in \mathcal{V}$ fulfill the coupling conditions (3.6) and (3.7). Moreover, V_i^* is connected to V_i^o by an incoming Lax curve along the respective pipe. The neighborhood can be chosen sufficiently small, such that the corresponding states are subsonic.

A similar result holds true in the case of the compressor condition (2.15) for any given value $CR > 0$.

Proof. Denote by $M = |I^-| + |I^+|$ the total number of connected pipes. For $V := (V_i)_{i\in I^\pm} := (K_i, L_i)_{i\in I^\pm}$ the coupling conditions (3.6) and (3.7) are given by the function $\Psi : \mathbb{R}^{2M} \times \mathbb{R}^{2M} \times \mathbb{R}^M \to \mathbb{R}^M$.

$$\Psi(V, (V^o, R^o)) := \begin{bmatrix} \sum_{i\in I^-} A_i K_i - \sum_{j\in I^+} A_j K_j \\ P(V_1) - P(V_2) \\ \vdots \\ P(V_{M-1}) - P(V_M) \end{bmatrix} \tag{3.12}$$

where P is defined in equation (3.7). By assumption we have $\Psi(\widehat{V}, (\widehat{V}, \widehat{R})) = 0$. Now, we define

$$\overline{\Psi}(\sigma, (V^o, R^o)) := \Psi(\overline{V}(\sigma), (V^o, R^o)) : \mathbb{R}^M \times \mathbb{R}^{2M} \times \mathbb{R}^M \to \mathbb{R}^M$$

where

$$\overline{V}(\sigma) := (\overline{V}_i(\sigma_i))_{i\in I^\pm}$$

and the components of $\overline{V}_i(\sigma_i)$ are given by equation (3.9) and equation (3.10), respectively. Further, $\sigma = (\sigma_i)_{i\in I^\pm}$. Next, we compute the determinant of $D_\sigma \overline{\Psi}(\sigma, (V^o, R^o))$ at $\sigma = 0$. We have for $i \in I^-$ and $j \in I^+$

$$D_\sigma \overline{\Psi} = \begin{bmatrix} A_1 \frac{dK_1}{d\sigma_1} & \dots & A_i \frac{dK_{|I^-|}}{d\sigma_{|I^-|}} & \dots & -A_j \frac{dK_j}{d\sigma_j} & \dots & -A_{|I^+|} \frac{dK_{|I^+|}}{d\sigma_{|I^+|}} \\ \frac{dP_1}{d\sigma_1} & -\frac{dP_2}{d\sigma_2} & 0 & \dots & \dots & \dots & 0 \\ 0 & \frac{dP_2}{d\sigma_2} & -\frac{dP_3}{d\sigma_3} & 0 & \dots & \dots & 0 \\ & & \ddots & \ddots & & & \\ & & & & \ddots & \ddots & \\ 0 & \dots & \dots & \dots & 0 & \frac{dP_{M-1}}{d\sigma_{M-1}} & -\frac{dP_M}{d\sigma_M} \end{bmatrix} \tag{3.13}$$

and therefore

$$det(D_\sigma \overline{\Psi}) = (-1)^{M-1} \sum_{i\in I^-} \Big(A_i \frac{dK_i}{d\sigma_i} \prod_{k\in I^-, k\neq i} \frac{dP_k}{d\sigma_k} \Big) + (-1)^M \sum_{j\in I^+} \Big(A_j \frac{dK_j}{d\sigma_j} \prod_{k\in I^-, k\neq j} \frac{dP_k}{d\sigma_k} \Big), \tag{3.14}$$

$$\frac{dP_i}{d\sigma_i} = \frac{1}{2} \left(\frac{dL_i}{d\sigma_i} + \frac{(L_i - R_i)\frac{dL_i}{d\sigma_i} - 4a^2 K_i \frac{dK_i}{d\sigma_i}}{\sqrt{(L_i - R_i)^2 - 4a^2 K_i^2}} \right).$$

From equations (3.9) and (3.10), we obtain at $\sigma_i = 0$

$$\begin{aligned} &\frac{dK_i}{d\sigma_i}(0) = q_l - a\rho_l < 0, \quad \frac{dL_i}{d\sigma_i}(0) = \frac{(q_l - a\rho_l)^2}{\rho_l} \neq 0, \forall i \in I^-, \\ &\frac{dK_i}{d\sigma_i}(0) = q_r + a\rho_r > 0, \quad \frac{dL_i}{d\sigma_i}(0) = \frac{(q_r + a\rho_r)^2}{\rho_r} \neq 0, \forall i \in I^+. \end{aligned}$$

Hence, also $\frac{dP_i}{d\sigma_i}(\sigma_i = 0) = a^2 \rho_i^o \neq 0$ and therefore $detD_\sigma \overline{\Psi}(0, (V^o, R^o)) \neq 0$. By the implicit function theorem there exists an open neighborhood $\mathcal{V}$ of $\widehat{V}$ such that for all initial data $V^o \in \mathcal{V}$ there exists σ^* such that $V^* := \bar{V}(\sigma^*)$ fulfills the coupling conditions, i.e.

$$\Psi(V^*, (V^o, R^o)) = \overline{\Psi}(\sigma^*, (V^o, R^o)) = 0.$$

Since the corresponding state of $\widehat{V}$ in conservative variables is strictly subsonic we may assume, by possibility decreasing the size of $\mathcal{V}$, that also the conservative variables corresponding to (V^*, R^o) are subsonic. □

Remark 3.2. *Note that we have omitted the source term when computing the solution along the Lax curves. This is justified by the semi-discrete formulation of the finite volume scheme in the next section, which implies that we are evaluating the coupling condition at a set of measure zero in space-time. Since the source term is bounded, it does not contribute to the integral over the cells.*

Remark 3.3. *Another possibility is to reformulate system* (3.1) *as a system of three equations in* (K_i, L_i, R_i) *with the equation for* R_i *given by*

$$\partial_t R_i = 0.$$

Therefore, the corresponding hyperbolic field has a zero eigenvalue in an independent subspace. This yields a characteristic boundary at each adjacent pipe. Hence in phase space, at each pipe i *any value* $\tilde{R}_i$ *can be connected along a wave curve to* R_i *leads to a contact discontinuity of zero velocity at the nodal point. Hence, the trace of* R_i *at* $x = x_o$ *is independent of* $\tilde{R}_i$*.*

4 A Well-balanced Central Upwind Scheme For Nodal Dynamics

We compute the evolution of the conservative variables using the second–order central upwind scheme [11, 24, 25]. The computational domain Ω_i is discretized in cells $[x_{j-\frac{1}{2}}, x_{j+\frac{1}{2}}]$ of size Δx and centered at $x_j = \bar{x} + (j - \frac{1}{2})\Delta x$ for $j = 1, \dots, N$. We choose $\bar{x}$ such that $x_N = x_o$ for $i \in I^-$ and $x_0 = x_o$ for $i \in I^+$. For simplicity the same number of cells N for all adjacent pipes will be used. The approximated cell averages at fixed time t are computed as

$$U_i^j(t) := \frac{1}{\Delta x} \int_{x_{j-\frac{1}{2}}}^{x_{j+\frac{1}{2}}} U_i(x,t)dx, , \ i \in I^{\pm}, j = 1, \dots, N.$$

The evolution of conservative variables, density and momentum using central upwind scheme [24, 25] reads

$$\frac{dU_i^j}{dt} = -\frac{\mathcal{V}_i^{j+1/2} - \mathcal{V}_i^{j-1/2}}{\Delta x} \tag{4.1}$$

where $\mathcal{V}_i^{j-1/2}, \mathcal{V}_i^{j+1/2}$ are the fluxes across the left and right interface of cell j, respectively. At the junction, the flux is the new trace of the equilibrium variable,

$$\mathcal{V}_i^{N+1/2} = V_i^*, i \in I^-, \tag{4.2}$$

$$\mathcal{V}_i^{1/2} = V_i^*, i \in I^+. \tag{4.3}$$

The new traces V_i^* are constructed with the help of Lemma 3.1 based on the old traces $V_i^{N,E}, i \in I^-$ and $V_i^{1,W}, i \in I^+$. The point values of K and L at the cell interfaces, i.e.,

$K_i^{j,E}, K_i^{j,W}, L_i^{j,E}, L_i^{j,W}$, are computed using piecewise linear reconstruction of K_i^j and L_i^j calculated using the cell averages (ρ_i^j, q_i^j) using equation (3.3). The values R_i are computed using a second–order quadrature rule applied to the integral starting for example at $\tilde{x} = x_o$ with $R_i = 0$ at each pipe according to the following equations

$$R_i^{1/2} = R_k^{N+1/2} = 0 \quad \forall i \in I^+, k \in I^-,$$
$$R_i^{j+1/2} = R_i^{j-1/2} + \Delta x \frac{f_{g,i}}{2D_i} \frac{q_i^j |q_i^j|}{\rho_i^j},\ R_k^{j-1/2} = R_k^{j+1/2} + \Delta x \frac{f_{g,k}}{2D_k} \frac{q_k^j |q_k^j|}{\rho_k^j}.$$

i.e., for $W \in \{K, L\}$,

$$W_i^{j,E} = W_i^j + \frac{\Delta x}{2}(W_x)_i^j,\ W_i^{j,W} = W_i^j - \frac{\Delta x}{2}(W_x)_i^j \tag{4.4}$$

with numerical derivatives

$$(W_x)_i^j = \begin{cases} \frac{W_i^{j+1} - W_i^j}{\Delta x}, & j = 1 \\ \frac{W_i^j - W_i^{j-1}}{\Delta x}, & j = N \\ \mathbf{minmod}\Big(\theta \frac{W_i^{j+1} - W_i^j}{\Delta x}, \frac{W_i^{j+1} - W_i^{j-1}}{2\Delta x}, \theta \frac{W_i^j - W_i^{j-1}}{\Delta x}\Big), & \text{otherwise,} \end{cases} \tag{4.5}$$

$\theta \in [1, 2]$ and minmod limiter

$$\mathbf{minmod}(w_1, w_2, \ldots, w_n) = \begin{cases} min(w_1, w_2, \ldots, w_n) & \text{if } w_i > 0,\ \forall i \\ max(w_1, w_2, \ldots, w_n) & \text{if } w_i < 0,\ \forall i \\ 0 & \text{otherwise} \end{cases} \tag{4.6}$$

For interior interfaces, we may use any conservative numerical flux functions whose numerical diffusion vanishes at equilibrium states. Here we choose the central upwind flux ,

$$\begin{aligned} \big(\mathcal{V}_i^{j+1/2}\big)^{(1)} &= \frac{a_{i,+}^{j+1/2} K_i^{j,E} - a_{i,-}^{j+1/2} K_i^{j+1,W}}{a_{i,+}^{j+1/2} - a_{i,-}^{j+1/2}} \\ &\quad + \alpha_i^{j+1/2} (\rho_i^{j+1,W} - \rho_i^{j,E}) \mathcal{H}\Big(\frac{|K_i^{j+1} - K_i^j|}{\Delta x} \frac{|\Omega|}{\max_j\{K_i^j\}}\Big), \end{aligned} \tag{4.7}$$

$$\begin{aligned} \big(\mathcal{V}_i^{j+1/2}\big)^{(2)} &= \frac{a_{i,+}^{j+1/2} L_i^{j,E} - a_{i,-}^{j+1/2} L_i^{j+1,W}}{a_{i,+}^{j+1/2} - a_{i,-}^{j+1/2}} \\ &\quad + \alpha_i^{j+1/2} (q_i^{j+1,W} - q_i^{j,E}) \mathcal{H}\Big(\frac{|L_i^{j+1} - L_i^j|}{\Delta x} \frac{|\Omega|}{\max_j\{L_i^j\}}\Big). \end{aligned} \tag{4.8}$$

where $|\Omega|$ is the size of computational domain, $a_{i,\pm}^{j+1/2}$ are the maximum and minimum eigenvalues of the Jacobian, i.e.,

$$a_{i,+}^{j+1/2} = \max\big(\lambda(U_i^{j,E}), \lambda(U_i^{j+1,W}), 0\big), \quad a_{i,-}^{j+1/2} = \min\big(\lambda(U_i^{j,E}), \lambda(U_i^{j+1,W}), 0\big) \tag{4.9}$$

and $\alpha_i^{j+1/2}$ is the local diffusion computed as $\alpha_i^{j+1/2} = \frac{a_{i,+}^{j+1/2} a_{i,-}^{j+1/2}}{a_{i,+}^{j+1/2} - a_{i,-}^{j+1/2}}$.

Note that the numerical diffusion of the standard HLL-flux (obtained for $\mathcal{H} = 1$) would not give a well-balanced scheme, because the numerical diffusion of the mass flux is written in terms of differences of the conservative variables and not the equilibrium variables. The additional limiter $\mathcal{H}$ turns off the numerical diffusion as we approach the equilibrium state. For some positive $C > 0$ and $m > 0$, it is given by

$$\mathcal{H}(z) = \frac{(Cz)^m}{1 + (Cz)^m}. \tag{4.10}$$

In the interior of the domain the previously defined flux preserves steady state: In steady state we obtain $K_i^{j,E} = K_i^{j+1,W} = K_i^j = const$ and similarly for L_i^j. Hence, we obtain $\mathcal{H} = 0$ and therefore $\mathcal{V}_i^{j+1/2} - \mathcal{V}_i^{j-1/2} = 0$ and the steady state is preserved.

Lemma 4.1. *The numerical scheme given by* (4.1) *and flux defined by* (4.7) *preserves the steady state across a node of M adjacent pipes and coupling conditions given by* (3.6) *and* (3.7).

Proof. Consider steady state $(\widehat{V}, \widehat{R}) := (\widehat{V}_i, \widehat{R}_i)_{i \in I^\pm}$. Then all numerical derivatives in (4.5) as well as the numerical diffusion terms vanish. Thus the numerical fluxes are given by $\mathcal{V}_i^{j+1/2} = \widehat{V}_i$ for all $j = 2, \ldots, N-1$. At the nodal point the flux variables satisfy the coupling conditions (3.6) and (3.7). Then, the boundary data K_i^* and L_i^* are obtained according to Lemma 3.1. Since the states are unique we obtain $K_i^j = K_i^* = \widehat{K}_i$ and $L_i^j = L_i^* = \widehat{L}_i$ and hence the boundary fluxes for each pipe at the junction are $\mathcal{V}_i^{N+1/2} = \mathcal{V}_i^{N-1/2} = (\widehat{K}_i, \widehat{L}_i)^T$ for incoming pipes $i \in I^-$ and $\mathcal{V}_i^{1/2} = \mathcal{V}_i^{3/2} = (\widehat{K}_i, \widehat{L}_i)^T$ for outgoing pipes $j \in I^+$. Hence, the scheme is well–balanced across the node. □

Data: Given discretized initial conditions $U_i^j(0) = U_i(x, 0)$
while *terminal time not reached* **do**
  Compute equilibrium variables (K_i^j, L_i^j, R_i^j) by (3.3) ;
  Reconstruct the values of K and L at the cell interface by (4.4) ;
  Solve the coupling conditions,(3.6),(3.7) to find K_i^*, L_i^* Calculate conservative variables (ρ, q) at the cell interface by equations (3.4) ;
  Calculate fluxes (4.7) for interior cell boundaries and use K_i^*, L_i^* at junction ;
  Compute the time step $\Delta t = \frac{CFL\Delta x}{\max_{i,j} |\lambda_i^j|}$ where λ_i^j is the maximal eigenvalue of the Jacobian in cell j and pipe i;
  Evolve the conservative cell averages (4.1).
end

Some remarks are in order. The algorithm uses the same time step for all adjacent pipes. This is not necessary but simplifies the computation of the coupling condition. Also, the algorithm is second–order in the pipe but it may reduce to first order at the coupling condition. The algorithm can be extended to second–order across the nodal point using techniques presented in [2]. However, note that the steady state is constant and therefore the scheme preserves the steady state to any order across the nodal point.

5 Numerical Tests

In this section, we test the well-balanced(WB) scheme with numerical examples for steady state and near steady state flows. The results of this WB method have been compared with a second order non well-balanced method(NWB). The NWB scheme is given by,

$$\frac{dU_i^j}{dt} = -\frac{\mathcal{F}_i^{j+1/2} - \mathcal{F}_i^{j-1/2}}{\Delta x} + \mathcal{S}_i^j \tag{5.1}$$

where $\mathcal{F}$ is the HLL flux given by,

$$\mathcal{F}_i^{j+1/2} = \frac{a_{i,+}^{j+1/2} F(U_i^{j,E}) - a_{i,-}^{j+1/2} F(U_i^{j+1,W})}{a_{i,+}^{j+1/2} - a_{i,-}^{j+1/2}} + \alpha_i^{j+1/2}(U_i^{j+1,W} - U_i^{j,E})$$

where the flux terms are as defined in (1.2) and $\mathcal{S}_i^j$ is the source term given in (1.2) at the point U_i^j. The coupling conditions (2.12), (2.13) are used to calculate the density and momentum at a node. The coupling conditions at the node are solved with Newton's methd for both WB and NWB scheme.

The parameters used in the WB scheme are $\theta = 1$, C=100, m=1 and CFL number=0.4. All the pipes in the examples have been considered to be of same diameter and friction factor, $\frac{f_g}{2D} = 1$ and the speed of sound for the gas, $a = 1$. We compute several well-balanced flows at junctions and compressors, as well as perturbations of such steady states.

5.1 Steady state at a node

In this example, we study the WB scheme for a steady state at a node with three types of pipe combinations–one incoming and 1 outgoing pipes; 1 incoming and 2 outgoing pipe; and 2 incoming and 1 outgoing pipe. The initial conditions are selected in such a way that the node is at steady state with the equilibrium variables constant in each pipe and satisfying the coupling conditions at the node.

The initial condition for first case with one incoming and outgoing pipe are $K_1 = K_2 = 0.15$ and $p^* = 0.332$ corresponding to $L_1 = L_2 = 0.4$. Similarly for the second case, of 1 incoming and 2 outgoing pipe, $K_1 = 0.15, K_2 = K_3 = 0.075$ and $p^* = 0.332$ or $L_1 = 0.4, L_2 = L_3 = 0.3492$; and for 2 incoming and 1 outgoing pipes, $K_3 = 0.15, K_1 = K_2 = 0.075$ and $p^* = 0.332$ or $L_3 = 0.4, L_1 = L_2 = 0.3492$.

The L-1 error for the three cases is given in the table below, As can be seen from the results in Table 1, the L-1 error $||K - \widehat{K}||$ and $||L - \widehat{L}||$ is upto machine precision using the WB scheme. Whereas it is of the order of 10^{-7} to 10^{-8} with the NWB scheme. We can also note that the coupling conditions in terms of (K,L) converge quickly using Newton's method and do not affect the well-balancing property of the scheme at the node.

5.2 Steady state with a compressor

In the second example, we study the well balancing at steady state for compressor connecting two pipes with compression ratios $CR = 1.5, 2, 2.5$. The initial conditions are selected in a

No. of cells in each pipe	L1-error for variable	1 Incoming, 1 Outgoing		1 Incoming, 2 Outgoing		2 Incoming, 1 Outgoing	
		WB	NWB	WB	NWB	WB	NWB
50	K	$2.94\text{x}10^{-17}$	$6.19\text{x}10^{-7}$	$6.74\text{x}10^{-17}$	$3.78\text{x}10^{-7}$	$6.91\text{x}10^{-17}$	$3.45\text{x}10^{-7}$
	L	$3.22\text{x}10^{-17}$	$9.48\text{x}10^{-7}$	$5.88\text{x}10^{-17}$	$3.57\text{x}10^{-7}$	$5.77\text{x}10^{-17}$	$7.38\text{x}10^{-7}$
100	K	$8.74\text{x}10^{-17}$	$1.56\text{x}10^{-7}$	$1.30\text{x}10^{-16}$	$9.63\text{x}10^{-8}$	$1.14\text{x}10^{-16}$	$8.67\text{x}10^{-8}$
	L	$1.27\text{x}10^{-16}$	$2.43\text{x}10^{-7}$	$7.74\text{x}10^{-17}$	$8.94\text{x}10^{-8}$	$8.30\text{x}10^{-17}$	$1.87\text{x}10^{-7}$
200	K	$5.59\text{x}10^{-17}$	$3.88\text{x}10^{-8}$	$1.09\text{x}10^{-16}$	$2.62\text{x}10^{-8}$	$1.25\text{x}10^{-16}$	$2.69\text{x}10^{-8}$
	L	$7.05\text{x}10^{-17}$	$6.13\text{x}10^{-8}$	$1.13\text{x}10^{-16}$	$2.32\text{x}10^{-8}$	$1.12\text{x}10^{-16}$	$5.03\text{x}10^{-8}$

Table 1: Comparison of L-1 errors between well-balanced(WB) and non well-balanced(NWB) scheme at steady state for a junction at time T=1

way that the compressor is at steady state for time,T=0. The momentum in the two pipes is given by $K_1 = K_2 = 0.15$ and pressure is given by $p_1^* = 0.332$ and $p_2^* = CRp_1^*$. The L1 errors using the WB and NWB scheme are given in the table below. Similar to the first example,

No. of cells in each pipe	L1-error for variable	CR=1.5		CR=2.0		CR=2.5	
		WB	NWB	WB	NWB	WB	NWB
50	K	$1.75\text{x}10^{-17}$	$4.16\text{x}10^{-7}$	$6.74\text{x}10^{-17}$	$3.78\text{x}10^{-7}$	$2.33\text{x}10^{-17}$	$3.77\text{x}10^{-7}$
	L	$2.72\text{x}10^{-17}$	$4.00\text{x}10^{-7}$	$5.88\text{x}10^{-16}$	$3.57\text{x}10^{-7}$	$1.39\text{x}10^{-17}$	$3.54\text{x}10^{-7}$
100	K	$3.91\text{x}10^{-17}$	$1.05\text{x}10^{-7}$	$1.30\text{x}10^{-16}$	$9.63\text{x}10^{-8}$	$4.72\text{x}10^{-16}$	$9.68\text{x}10^{-8}$
	L	$5.59\text{x}10^{-16}$	$1.01\text{x}10^{-7}$	$7.74\text{x}10^{-17}$	$8.94\text{x}10^{-8}$	$3.61\text{x}10^{-17}$	$8.89\text{x}10^{-7}$
200	K	$5.32\text{x}10^{-17}$	$2.64\text{x}10^{-8}$	$1.09\text{x}10^{-16}$	$2.62\text{x}10^{-8}$	$1.08\text{x}10^{-16}$	$2.84\text{x}10^{-8}$
	L	$5.88\text{x}10^{-17}$	$2.53\text{x}10^{-8}$	$1.13\text{x}10^{-16}$	$2.32\text{x}10^{-8}$	$1.19\text{x}10^{-16}$	$2.59\text{x}10^{-8}$

Table 2: Comparison of L-1 errors between well-balanced(WB) and non well-balanced(NWB) scheme at steady state with a compressor at different compression ratios at time T=1

we see that the L1 errors using the WB scheme are accurate upto machine precision. Also the coupling conditions for the compressor do not affect the well-balancing of the scheme.

5.3 Perturbations to steady state for a node

From the first two examples, we can see that the WB scheme preserves steady state. In this example we will compare the results from the WB and NWB scheme for perturbations to the momentum at steady state. The initial conditions for the perturbed state are given by,

$$K_i(x) = \widehat{K}_i + \eta_i e^{-100(x-x_0)^2},\ L_i = \widehat{L}_i\ \forall i = 1, 2 \dots M \tag{5.2}$$

where $\widehat{K}_i$ and $\widehat{L}_i$ are constant steady state equilibrium variables in the two pipes and η_i is the magnitude of perturbation at the node.

At first, we consider a node connecting two pipes. The equilibrium variables for this case are given by, $\widehat{K}_i = 0.15$ and $\widehat{L}_i = 0.4$. At first we consider perturbation of $\eta_i = 10^{-3}$ at the junction. The momentum at time T=0.2 are as shown in figure below,

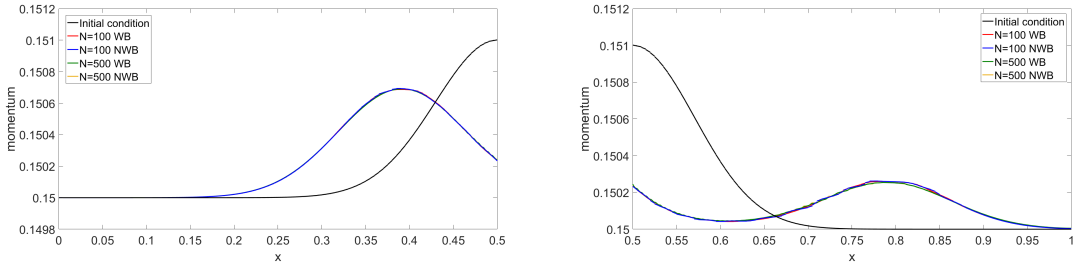

(a) First Pipe (b) Second Pipe

Figure 3: Momentum for perturbation of order 10^{-3} for a node connected to two pipes

We can see from the results that both the WB and NWB schemes provide similar solutions for the perturbation of order 10^{-3} at the node. We now reduce this perturbation to $\eta_i = 10^{-6}$.

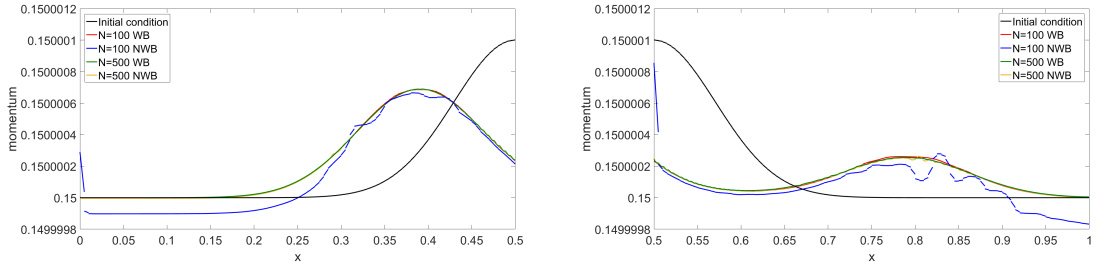

(a) First Pipe (b) Second pipe

Figure 4: Momentum for perturbation of order 10^{-6} for a node connected to two pipes

From Figure 4 we can see that NWB scheme develops oscillations for N=100 when the perturbation of order 10^{-6}. The perturbation is resolved better for a finer grid with N=500 per pipe. However in the case of WB method, the scheme is able to capture the perturbations well even for a coarser grid of N=100 per pipe.

We now do a similar test for a node connected to 1 incoming and 2 outgoing pipes. The equilibrium state are given by, $\widehat{K}_1 = 0.15, \widehat{K}_2 = \widehat{K}_3 = 0.075$ and $\widehat{L}_1 = 0.4, \widehat{L}_2 = \widehat{L}_3 = 0.3492$. Like the previous example we run the simulation for two perturbations upto a time T=0.2. Figure 5 shows the result for momentum with $\eta_1^* = 10^{-3}, \eta_2^* = \eta_3^* = 0.5\text{x}10^{-3}$ and Figure 6 for $\eta_1^* = 10^{-6}, \eta_2^* = \eta_3^* = 0.5\text{x}10^{-6}$ respectively.

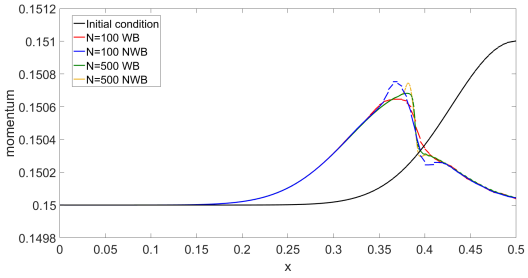

(a) First pipe

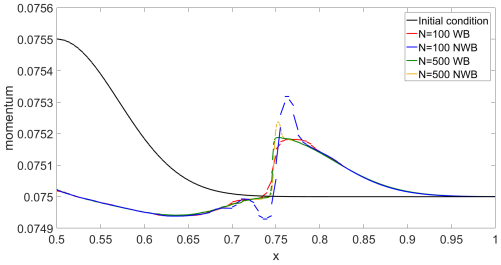

(b) Second pipe

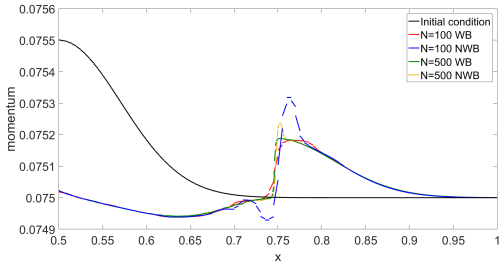

(c) Third pipe

Figure 5: Momentum for perturbation of order 10^{-3} for a node connected to one incoming and two outgoing pipes

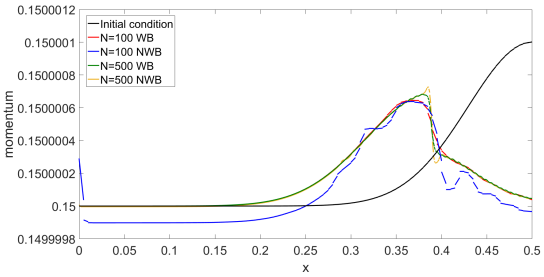

(a) First pipe

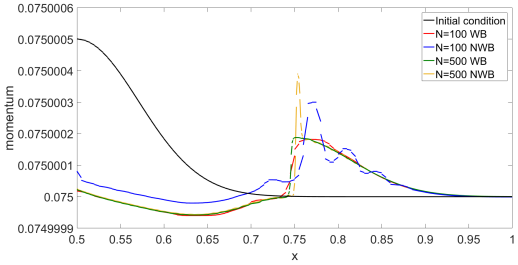

(b) Second pipe

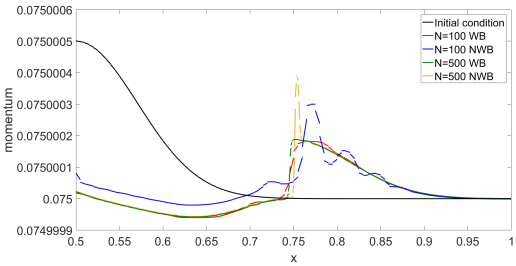

(c) Third pipe

Figure 6: Momentum for perturbation of order 10^{-6} for a node connected to one incoming and two outgoing pipes

We see from the results that even for the perturbations of order 10^{-3}, the results from NWB scheme are unstable where there is a sharp increase in momentum. The results of NWB

scheme are even more oscillatory when the perturbations are of order 10^{-6}. Further even with a finer resolution, we can see a spike in the region where there is sharp increase of momentum. However, these issues are resolved with the WB scheme. The results of WB scheme with coarser grid are a little more diffusive than the finer grid, but there are no instabilities arising in the results.

6 Conclusion

In this paper we have extended a well-balanced scheme, developed by Chertock, Herty and Özcan [11] for one-dimensional systems, to a network of gas pipelines with friction. In particular we looked at intersections of pipes at a node and compressors within a pipeline network. We prove well-posedness and well-balancing of the new scheme. For compressors and for junctions of three pipes, numerical experiments demonstrate that equilibria are resolved up to machine accuracy. Most interestingly, near equilibrium flows are resolved robustly and accurately, even in cases where a standard non-balanced scheme fails.

Acknowledgments

This work has been supported by HE5386/13–15, BMBF ENets Project, and DFG Research Training Group 2326 Energy, Entropy, and Dissipative Dynamics, RWTH Aachen University.

References

[1] E. Audusse, F. Bouchut, M.-O. Bristeau, R. Klein, and B. t. Perthame, *A fast and stable well-balanced scheme with hydrostatic reconstruction for shallow water flows*, SIAM J. Sci. Comput., 25 (2004), pp. 2050–2065.

[2] M. K. Banda, A.-S. Häck, and M. Herty, *Numerical discretization of coupling conditions by high-order schemes*, J. Sci. Comput., 69 (2016), pp. 122–145.

[3] M. K. Banda, M. Herty, and A. Klar, *Coupling conditions for gas networks governed by the isothermal Euler equations*, Netw. Heterog. Media, 1 (2006), pp. 295–314.

[4] ——, *Gas flow in pipeline networks*, Netw. Heterog. Media, 1 (2006), pp. 41–56.

[5] A. Bermúdez, X. López, and M. E. Vázquez-Cendón, *Treating network junctions in finite volume solution of transient gas flow models*, J. Comput. Phys., 344 (2017), pp. 187–209.

[6] A. Bollermann, G. Chen, A. Kurganov, and S. Noelle, *A well-balanced reconstruction of wet/dry fronts for the shallow water equations*, J. Sci. Comput., 56 (2013), pp. 267–290.

[7] R. Borsche and J. Kall, *ADER schemes and high order coupling on networks of hyperbolic conservation laws*, J. Comput. Phys., 273 (2014), pp. 658–670.

[8] A. Bressan, S. Čanić, M. Garavello, M. Herty, and B. Piccoli, *Flows on networks: recent results and perspectives*, EMS Surv. Math. Sci., 1 (2014), pp. 47–111.

[9] J. Brouwer, I. Gasser, and M. Herty, *Gas pipeline models revisited: model hierarchies, nonisothermal models, and simulations of networks*, Multiscale Model. Simul., 9 (2011), pp. 601–623.

[10] G. Chen and S. Noelle, *A new hydrostatic reconstruction scheme based on subcell reconstructions*, SIAM J. Numer. Anal., 55 (2017), pp. 758–784.

[11] A. Chertock, M. Herty, and S. N. Özcan, *Well-balanced central-upwind schemes for 2x2 system of balance laws*, Proceedings of the XVI International Conference on Hyperbolic Problems, Springer(accepted), (2017).

[12] R. M. Colombo and M. Garavello, *A well posed Riemann problem for the p-system at a junction*, Netw. Heterog. Media, 1 (2006), pp. 495–511.

[13] ——, *On the Cauchy problem for the p-system at a junction*, SIAM J. Math. Anal., 39 (2008), pp. 1456–1471.

[14] R. M. Colombo, G. Guerra, M. Herty, and V. Schleper, *Optimal control in networks of pipes and canals*, SIAM J. Control Optim., 48 (2009), pp. 2032–2050.

[15] R. M. Colombo, M. Herty, and V. Sachers, *On* 2×2 *conservation laws at a junction*, SIAM J. Math. Anal., 40 (2008), pp. 605–622.

[16] R. M. Colombo and C. Mauri, *Euler system for compressible fluids at a junction*, J. Hyperbolic Differ. Equ., 5 (2008), pp. 547–568.

[17] R. Courant and K. O. Friedrichs, *Supersonic Flow and Shock Waves*, Interscience Publishers, Inc., New York, N. Y., 1948.

[18] S. A. Dyachenko, A. Zlotnik, A. O. Korotkevich, and M. Chertkov, *Operator splitting method for simulation of dynamic flows in natural gas pipeline networks*, Phys. D, 361 (2017), pp. 1–11.

[19] E. Godlewski, K.-C. Le Thanh, and P.-A. Raviart, *The numerical interface coupling of nonlinear hyperbolic systems of conservation laws. II. The case of systems*, M2AN Math. Model. Numer. Anal., 39 (2005), pp. 649–692.

[20] M. Gugat, M. Herty, and S. Müller, *Coupling conditions for the transition from supersonic to subsonic fluid states*, Netw. Heterog. Media, 12 (2017), pp. 371–380.

[21] M. Gugat and S. Ulbrich, *The isothermal Euler equations for ideal gas with source term: product solutions, flow reversal and no blow up*, J. Math. Anal. Appl., 454 (2017), pp. 439–452.

[22] M. Herty, J. Mohring, and V. Sachers, *A new model for gas flow in pipe networks*, Math. Methods Appl. Sci., 33 (2010), pp. 845–855.

[23] M. Herty and M. Seaï d, *Simulation of transient gas flow at pipe-to-pipe intersections*, Internat. J. Numer. Methods Fluids, 56 (2008), pp. 485–506.

[24] A. Kurganov and E. Tadmor, *New high-resolution central schemes for nonlinear conservation laws and convection-diffusion equations*, J. Comput. Phys., 160 (2000), pp. 241–282.

[25] ——, *Solution of two-dimensional Riemann problems for gas dynamics without Riemann problem solvers*, Numer. Methods Partial Differential Equations, 18 (2002), pp. 584–608.

[26] A. Morin and G. A. Reigstad, *Pipe networks: Coupling constants in a junction for the isentropic euler equations*, Energy Procedia, 64 (2015), pp. 140–149.

[27] A. Naumann, O. Kolb, and M. Semplice, *On a third order CWENO boundary treatment with application to networks of hyperbolic conservation laws*, Appl. Math. Comput., 325 (2018), pp. 252–270.

[28] S. Noelle, N. Pankratz, G. Puppo, and J. R. Natvig, *Well-balanced finite volume schemes of arbitrary order of accuracy for shallow water flows*, J. Comput. Phys., 213 (2006), pp. 474–499.

[29] S. Noelle, Y. Xing, and C.-W. Shu, *High-order well-balanced finite volume WENO schemes for shallow water equation with moving water*, J. Comput. Phys., 226 (2007), pp. 29–58.

[30] A. Osiadacz, *Nonlinear programming applied to the optimum control of a gas compressor station*, Internat. J. Numer. Methods Engrg., 15 (1980), pp. 1287–1301.

[31] G. Puppo and G. Russo, eds., *Numerical methods for balance laws*, vol. 24 of Quaderni di Matematica [Mathematics Series], Department of Mathematics, Seconda Università di Napoli, Caserta, 2009.

[32] G. A. Reigstad, *Numerical network models and entropy principles for isothermal junction flow*, Netw. Heterog. Media, 9 (2014), pp. 65–95.

[33] ——, *Existence and uniqueness of solutions to the generalized Riemann problem for isentropic flow*, SIAM J. Appl. Math., 75 (2015), pp. 679–702.

[34] G. A. Reigstad, T. Flåtten, N. Erland Haugen, and T. Ytrehus, *Coupling constants and the generalized Riemann problem for isothermal junction flow*, J. Hyperbolic Differ. Equ., 12 (2015), pp. 37–59.